Reaction coordinates and transition pathways of rare events via forward flux sampling

Ernesto E. Borrero and Fernando A. Escobedo
School of Chemical and Biomolecular Engineering, Cornell University, Ithaca, New York 14853, USA

(Received 21 May 2007; accepted 2 August 2007; published online 22 October 2007)

A new approach is developed for identifying suitable reaction coordinates to describe the progression of rare events in complex systems. The method is based on the forward flux sampling (FFS) technique and standard least-square estimation (LSE) and it is denoted as FFS-LSE. The FFS algorithm generates trajectories for the transition between stable states as chains of partially connected paths, which can then be used to obtain "on-the-fly" estimates for the committor probability to the final region, p_B. These p_B data are then used to screen a set of candidate collective properties for an optimal order parameter (i.e., reaction coordinate) that depends on a few relevant variables. LSE is used to find the coefficients of the proposed reaction coordinate model and an analysis of variance is used to determine the significant terms in the model. The method is demonstrated for several test systems, including the folding of a lattice protein. It is shown that a simple approximation to p_B via a model linear on energy and number of native contacts is sufficient to describe the intrinsic dynamics of the protein system and to ensure an efficient sampling of pathways. In addition, since the p_B surface found from the FFS-LSE approach leads to the identification of the transition state ensemble, mechanistic details of the dynamics of the system can be readily obtained during a single FFS-type simulation without the need to perform additional committor simulations. © *2007 American Institute of Physics*. [DOI: 10.1063/1.2776270]

I. INTRODUCTION

For many processes in complex biological systems involving proteins, including folding, aggregation, adsorption, and transport driven through membranes, the kinetics of such rare events is often very difficult to simulate by a conventional straightforward molecular dynamics (MD) approach.[1,2] This is because the average waiting time between events is orders of magnitude longer than the accessible simulation time itself, and most of the computational effort is spent simulating the uninteresting waiting period between events. Even when coarse-grained protein lattice models are simulated with dynamic Monte Carlo (MC), the required number of independent simulations needed to obtain accurate transition rate constants is extremely large.[3] To overcome this problem, specialized techniques have been proposed such as the Bennett-Chandler (BC) method,[4,5] effective positive flux (EPF) formalism,[6] the Crooks and Chandler approach,[7] transition path sampling (TPS),[8–11] milestoning methods,[12] transition interface sampling (TIS),[13,14] partial path transition interface sampling (PPTIS),[15] and "forward flux sampling" (FFS)-type simulation schemes.[2] These approaches can be classified as either "reactive flux" methods or "path sampling" methods. Reactive flux methods are based on a two-step approach wherein (i) the free-energy profile as a function of a reaction coordinate is first determined from an initial simulation (e.g., via umbrella sampling or thermodynamic integration) and (ii) the transmission coefficient is calculated by firing dynamical trajectories from the top of the free-energy barrier (approximately the transition state diving surface) in a second independent simulation. There exist several techniques to determine the transmission coefficient such as the BC method,[16] the history-dependent BC,[16] and the EPF formalism,[6] which differ in the way that the trajectories fired from the top energy barrier are counted. In these reactive flux methods, an improper choice of reaction coordinate will affect the correctness and efficiency of the transmission coefficient calculation[17] (e.g., leading to very low coefficients). Moreover, these methods do not provide information about the transition path ensemble (TPE) or the transition state ensemble (TSE) to extract mechanistic details of the dynamics of the system.

Path sampling methods are based on an importance sampling of dynamical trajectories instead of the free-energy barrier and transmission coefficient calculations. For example, TPS samples the TPE by using a MC procedure that generates new paths by "shooting" forward and backward in time from already existing paths of a fixed length in systems exhibiting stable states (i.e., equilibrium systems). The estimation of the average transition rate constants within the framework of TPS requires the definition of an order parameter, which is used only to distinguish the two stable states, and the calculation of a correlation function of state populations in time by an umbrella sampling approach.[7–9] Other methods, such as the Crooks and Chandler approach, can be applied to nonequilibrium systems and rely on a methodology that resembles the TPS in generating new paths from old paths by changing the random number history.[7] In TIS (Ref. 14) and PPTIS,[15] the efficiency of the TPE sampling is improved via a series of interfaces in phase space that facilitate the generation of flexible transition path lengths by a TPS-like procedure. Milestoning methods[12] are very similar to PPTIS, but trajectories between interfaces are generated by assuming a

steady-state distribution at each interface (i.e., a strong Markovian condition), an assumption that limits their applicability. Finally, FFS-type simulation algorithms that do not require the knowledge of the phase-space density exist and can therefore be used for nonequilibrium systems with stochastic dynamics. Like TIS, FFS allows the computation of both rate constants and TPE by dividing the phase space between the initial and final regions into a series of interfaces. FFS relies on the generation of partial trajectories between interfaces, in which the crossing points at the next interface of successful trial runs are stored and used to initiate new partial pathways for the following interface.[1,2,18] The TPE is obtained by connecting sequentially generated partial paths between the interfaces. The rate constant for the stochastic system is given by the product of the flux of trajectories crossing the first interface and the probability that these trajectories subsequently reach the final state. Although a series of interfaces in the phase space is used as in other sampling techniques, no assumption is made about the distribution of paths at the interfaces,[2] i.e., trajectories are generated without assuming a steady-state distribution at each interface (or "memory loss" during transitions like in milestoning methods[12]). Moreover, in FFS, reactive trajectories are obtained without any requirement on their length as in TPS, creating more connected trajectories between the stable states than in TIS with the same amount of MD steps, without relying on a Markovian assumption as in PPTIS.[17] These advantages of FFS made it the method of choice for this study.

From path sampling simulations, one can obtain not only the TPE between stables states but also the TSE, which is often very difficult to simulate by conventional "brute-force" approaches.[3,8] The TPE thus generated provides a viable method for obtaining mechanistic details and rate constants for the dynamics of the stochastic system. Moreover, all of these transition path methods avoid many of the difficulties associated with existing reactive flux methods and do not require the specification of a good reaction coordinate. However, it has been reported that the efficiency of these sampling schemes is sensitive to the choice of order parameter.[17] Hence, the challenges of applying a FFS-type algorithm to complex biological systems include (i) determination of an adequate order parameter that allows the description of the transition state regions and (ii) assessment of efficiency and completeness of sampling. In this paper, we attempt to address these two points by presenting a simple approach that identifies an adequate reaction coordinate (i.e., order parameter) that leads to an efficient sampling in FFS-type simulations.

In high-dimensional complex systems, it is not a trivial task to find a good order parameter (i.e., a reaction coordinate) that quantifies progress along the reaction pathways and allows distinguishing the stable states of the system. The knowledge of the reaction coordinate is essential for the understanding of the dynamics of the rare event and for the efficiency of the sampling algorithm.[17] The reaction coordinate is closely related to the probability of a configuration x to commit to the final state B, i.e., the "committor probability" $p_B(x)$,[19] which quantifies the tendency of configuration x to relax to the basin of attraction B under the system's intrinsic dynamics. Clearly, configurations in the initial basin A have $p_B=0$, those in basin B have $p_B=1$, and those at the TS have $p_B=\frac{1}{2}$. Hence, p_B can be seen as a perfect reaction coordinate in the sense that it provides a quantitative description of the dynamic behavior of every state along a trajectory. However, to be of practical use, p_B should be related to a few collective variables that are functions of the configurations, and thus compress many atomistic details into physically important properties.[19]

In the conventional committor analysis,[11,19] a minimum number of fleeting trajectories, $N_{\min}$, are initiated from a starting configuration along one of the paths belonging to the TPE and outside of the initial region A. The probability of a state in the phase space to commit to the final region is therefore estimated from the fraction of paths that ends in state B. Unfortunately this procedure to estimate p_B is costly, requiring a huge computational effort because each p_B value requires on the order of $N_{\min}=10$ fleeting trajectories, each half as long as a reactive trajectory.[3,11] Furthermore, good statistics require hundreds of estimates for p_B histograms and analysis of $\geqslant 100$ trajectories in the TPE.[19] The difficulties and computational cost of the committor analysis have motivated recent attempts to systematize the search for reaction coordinates. However, the majority of these methods continue to use expensive histogram calculations[20–24] and mainly focus on improving the trial and error aspects of the p_B calculation. For example, Ma and Dinner proposed a method based on neural networks to determine the functional dependence of p_B on a set of coordinates and a genetic algorithm that selects the combination of inputs that yields the best fit via the estimation of p_B histograms.[22] Hummer introduced a new criterion for the TS as those points in configurational space with high probability $p(\mathrm{TP}|x)$ that equilibrium trajectories passing through them are reactive (i.e., connect stable state). The projection of $p(\mathrm{TP}|x)$ onto a good reaction coordinate should give a sharply peaked distribution, which can be used to choose among different candidate order parameters,[20,21] but it requires estimation of a $p(\mathrm{TP}|x)$ histogram for each iterative improvement of the reaction coordinate model.[20,21] Weinan *et al.*[24] identified isocommittor surfaces (a costly procedure) to find effective transition tubes inside which the reactive trajectories stay confined (e.g., regions within the tubes where $p_B\sim\frac{1}{2}$ define the TS). Maragliano *et al.*[23] combined a string method with a sampling technique to determine minimum free-energy paths (MFEPs). Their approach presumes that transitions are most likely to occur around the MFEP, and thus isocommittor surfaces are determined therein. However, this approach requires many iterations of the mean force and variable entanglement calculations.[23]

A recently proposed approach for calculating reaction coordinates is based on TPS and likelihood maximization.[19] This so-called maximum likelihood (ML) method screens a set of candidate collective variables for a good reaction coordinate that depends on a few relevant variables. This is achieved by using a method denoted "aimless shooting" to harvest independent realizations of p_B. A simple model for the reaction coordinate, e.g., a linear combination of the collective variables, is then assumed and used to calculate the

likelihood of the model given the shooting data. The Bayesian information criterion is used to determine significant variables for the reaction coordinate. At present, this ML method[19] and the one proposed by Maragliano *et al.*[23] are the only two approaches that do not rely on costly histograms.

Stimulated by the ML approach, we present in this article an alternative algorithm to obtain estimates for p_B "on the fly" from a FFS-type simulation. These p_B data are then used to fit a model for the reaction coordinate in terms of several collective variables. Standard least-squares estimation (LSE) is used to find the coefficients of the model and an analysis of variance (ANOVA) is used to determine the significant terms in the model. In this way, an optimized reaction coordinate that depends on a few relevant variables is obtained. Hereafter, we refer to this approach as the FFS-LSE method. Since the resulting model for the reaction coordinate corresponds to the p_B surface response, the TSE and hence the mechanistic details of the process can be readily obtained by only analyzing characteristics of the collective variables at the p_B contour of $\frac{1}{2}\pm\sigma$ (where σ is the desired level of statistical accuracy). Moreover, we show that the computational efficiency of the FFS method can be increased with the use of the optimized order parameter. We illustrate the application of the FFS-LSE method to several simple test systems, including the folding of a lattice protein model.

II. FFS-TYPE SIMULATIONS

By way of background, we start by briefly reviewing the formalism of FFS-type simulation schemes for calculating transition pathways, in particular, for the branched growth path sampling method.

The FFS-type algorithm estimates the rate constant of the process as an average rate of transitions from two well defined states A and B using an "effective positive flux" expression.[1,2,13,14,18] To this end, it employs a series of noninteresting interfaces $(n+1)$ between the initial (A) and final (B) regions $\{\lambda_0,\ldots,\lambda_n\}$ defined by one or a combination of order parameters (λ), such that $\lambda\geqslant\lambda_0$, $\lambda_n=\lambda_B$, and $\lambda_i>\lambda_{i-1}$ (λ increases monotonically as the interfaces $\lambda_0,\ldots,\lambda_n$ are crossed). The order parameter $\lambda(x)$ can be chosen such that the system has values $\lambda(x)\leqslant\lambda_A(x)$ in region A and $\lambda(x)\geqslant\lambda_B(x)$ in region B. Here, x denotes the coordinates of the phase space. Hence, the rate constant $k_{A\to B}$ for transitions from A to B can be calculated from the total average flux from A to B, which can be expressed as the product of a flux from A to λ_0, $\bar{\Phi}_{A,0}$, and the probability that a trajectory reaching λ_0 from A will reach B without returning to A, $P(\lambda_{n=B}|\lambda_0)$:[2,13,14]

$$k_{A\to B}=\frac{\bar{\Phi}_{A,0}}{\bar{h}_A}P(\lambda_{n=B}|\lambda_0). \tag{1}$$

Here, the factor h_A is a history-dependent function such that $h_A=1$ if the system was more recently in A than in B, and $h_A=0$ otherwise; $\bar{h}_A$ is the average fraction of the time that the system spends in the basin of attraction of A. $P(\lambda_{n=B}|\lambda_0)$ can be expressed as the product of conditional probabilities:

$$P(\lambda_{n=B}|\lambda_0)=\prod_{i=0}^{n-1}P(\lambda_{i+1}|\lambda_i), \tag{2}$$

where $P(\lambda_{i+1}|\lambda_i)$ is the probability that a trajectory that visits A and crosses λ_i for the first time will subsequently reach λ_{i+1} without returning to the initial region A.[2]

The rare paths (excursions or jumps between stable states in the free-energy landscape) are captured by performing MC sampling of trajectories between interfaces. Furthermore, the paths belonging to the TPE are generated such that any trajectory from A to B passes through each interface in turn. The transitions between interfaces are free to follow any possible path between A and B, including paths crossing previous interfaces several times. Three path sampling schemes have been proposed in the literature to generate transition paths including[1,2] (i) the "direct" forward flux sampling (DFFS), (ii) branched growth (BG) method, and (iii) rosenbluth method. Our FFS-LSE approach is based on the BG sampling scheme, which we implemented as described below.

The BG method is illustrated schematically in Fig. 1(a), where branched transition paths are generated one by one. In the first stage of the algorithm, a simulation is carried out in the basin of attraction of A. After an equilibration period, $\lambda(x)$ is monitored during the run in basin A and configurations crossing λ_0 are stored. This simulation is suspended when a large set of crossing points at λ_0 is generated (for a valid crossing, the system must have visited A just before that). In the second stage of the algorithm, a branched path is generated from a randomly chosen configuration at λ_0. This single configuration at λ_0 is used to initiate k_0 trial runs, which are continued until either reaching λ_1 or returning to the initial region. Each configuration ending in λ_1 is stored and used as a starting point for k_1 trial runs to λ_2 or back to A. This procedure is repeated until either the final region $\lambda_n=\lambda_B$ is reached or because no successful trials were generated at some intermediate interfaces λ_i. In our implementation, the points saved at each λ_i were written on disk to avoid memory overload. An estimate of $P(\lambda_{n=B}|\lambda_0)$ is obtained as the total number of branches that eventually reach λ_n divided by the total possible number of branches, i.e.,

$$P(\lambda_{n=B}|\lambda_0)=\frac{N_S^{(n-1)}}{\Pi_{i=0}^{n-1}k_i}. \tag{3}$$

A new branching path is then generated by randomly choosing another point at λ_0 and following the same procedure outlined above to get a new estimate of $P(\lambda_{n=B}|\lambda_0)$. The final estimate of $P(\lambda_{n=B}|\lambda_0)$ is then obtained from the average over all such paths. The flux $\bar{\Phi}_{A,0}/\bar{h}_A$ in Eq. (1) is obtained from the simulation run in basin A by dividing the total number of crossing configurations at λ_0 by the total length of this run.

The characteristic transition pathways are obtained beginning with the collection of trials which arrive at $\lambda_B=\lambda_n$ from λ_{n-1} and tracing back the sequence of connected partial paths which link them to region A. For a complete descrip-

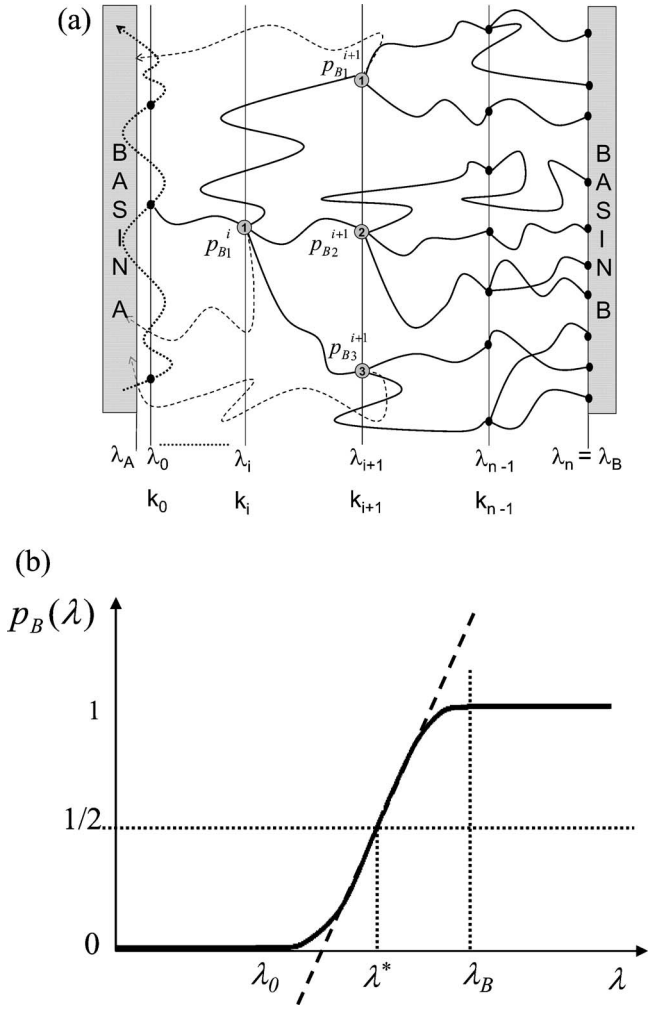

FIG. 1. (a) A schematic view of the generation of branched paths (thick lines) using the branched growth (BG) sampling method. The first stage involves the simulation run in the A basin shown by the dotted line. Starting points for the subsequent generation of branched paths are marked with the black circle at λ_0. The second stage corresponds to the trial runs (k_i) fired from λ_i; those that reached the next λ_{i+1} interface are shown by the thick line and those which failed to reach λ_{i+1} are shown by the dotted line. In this example, $k_i=4$, $k_{i+1}=3$, and $k_{i+2}=2$. $p_{Bj}^n=1$ for all points collected at $\lambda_{n=B}$. p_{Bj}^{i+1} for the points j at λ_{i+1} are estimated from Eq. (5) as follows: $p_{B1}^{i+1}=1/3[2/2+1/2]$, $p_{B2}^{i+1}=1/3[1/2+1/2+2/2]$, and $p_{B3}^{i+1}=1/3[1/2+2/2]$. The p_{B1}^i value for point 1 at λ_i is then obtained from $p_{B1}^i=3/4[p_{B1}^{i+1}+p_{B2}^{i+1}+p_{B3}^{i+1}]/3=1/4[1/2+2/3+1/2]$. (b) A sketch of the committor function $p_B(\lambda)$ in one dimension. $p_B\approx 0$ for points inside and near basin A because trajectories started thereof end in A; $p_B\approx 1$ for points in or near basin B because trajectories started thereof end in B. The statistical modeling of $p_B(\lambda)$ is restricted to the intermediate, transitional region of λ the dashed line illustrates a sample linear fit. The configurations for which $p_B(\lambda^*)\approx\frac{1}{2}$ are called transitions states.

tion of the theoretical background of the FFS-type algorithm and the path sampling schemes, we refer the readers to Ref. 2.

III. METHODS

A. p_B history from FFS-type simulation

As the trajectories harvested by FFS-type path sampling evolve in phase space, the stored points at each interface evolve in configuration space. Hence, each stored point has an intrinsic committor probability to reach the final region B. To extract p_B, the phase-space coordinates of the system must be stored for all points along all the trial runs which successfully reach λ_{i+1} from λ_i. One must also store information on the connectivity of the partial paths, i.e., by annotating each successful trial from λ_i to λ_{i+1} with an index that describes its initial point at λ_i. The BG scheme is ideal for tracking the p_B history, because from each stored point at λ_i one can estimate a p_B value from the outcome of the k_i branch generation trials started therein. Furthermore, the TPE is sampled with better resolution in the phase-space region close to TSE and B, where the transition paths are more branched.

The probability of each point at λ_i to reach the next interface λ_{i+1} before the initial region A, $p_j^i(\lambda_{i+1}|\lambda_i)$, can be easily obtained from

$$p_j^i(\lambda_{i+1}|\lambda_i)=\frac{N_j^i}{k_i}, \tag{4}$$

where N_j^i is the number of points reaching λ_{i+1} from point j at λ_i. The values of $p_j^i(\lambda_{i+1}|\lambda_i)$ are then used to calculate the B-committor probability of point j at λ_i, p_{Bj}^i:

$$p_{Bj}^i=p_j^i(\lambda_{i+1}|\lambda_i)\frac{\Sigma_{m=1}^{N_j^i}p_{Bm}^{i+1}}{N_j^i}=\frac{\Sigma_{m=1}^{N_j^i}p_{Bm}^{i+1}}{k_i}. \tag{5}$$

Equation (5) states that the p_{Bj}^i of point j at λ_i can be expressed as the product of the probability $p_j^i(\lambda_{i+1}|\lambda_i)$ that a trajectory initiated from this point reaches λ_{i+1} and the average p_{Bj}^{i+1} of all points at λ_{i+1} that connect with that state j at λ_i. Once the FFS-type simulation is complete, p_{Bj}^i values are obtained by following the trials that reached B back to λ_{n-1}, then following their connected partial paths back to λ_{n-2}, and so on back to A. As illustrated in Fig. 1(a), each point at λ_n has $p_{Bj}^n=1$. For each point at λ_{n-1}, the committor probability to B is simply given by $p_{Bj}^{n-1}=p_j^{n-1}(\lambda_n|\lambda_{n-1})$. Then, p_{Bj}^{n-1} values at λ_{n-1} are used to estimate p_{Bj}^{n-2} at λ_{n-2} using Eq. (5), and so on back to A. The FFS-type scheme distributes points in the full range of p_B values, and any reaction coordinate obtained from the p_B history will apply at every p_B along the transition pathways.

B. Reaction coordinate from p_B history

In general, we are interested in constructing the best possible reaction coordinates from a few collective variables. Therefore, the goal is to identify the simplest order parameter that not only measures the progress of the reaction but is also useful in characterizing the reaction dynamics. Simple reaction coordinates are better for the description of the system's dynamics, but the challenge is to determine which variables are important. Our strategy is to propose m candidate collective variables from which the model is constructed. The model is first tested to determine the variables that are significant for the fitting of the p_B data. These variables are then used to construct a second simpler model. In other words, this algorithm finds the best reaction coordinate as a function of a few candidate variables that are significantly correlated with p_B.

The approach presented here is related to the ML method recently proposed by Peters and Trout[19] for obtaining reac-

tion coordinates but we use a different method for sampling p_B (FFS rather than TPS) and for finding the model (LSE rather than ML, though LSE is a type of ML estimation). It is, however, beyond the scope of this work to compare the performance of both methods. The basis of both approaches is that p_B can serve as a guide to search efficiently the space of physically meaningful variables. Our method begins by harvesting an ensemble of typical trajectories for the transition between two stable states. This ensemble is obtained from a FFS-type simulation using an initial guess for the order parameter. As described in Sec. III A, the p_B value for each of the points crossing the interfaces is extracted from their path connectivity. Reaction coordinate candidates are then tested based on this p_B history by fitting the p_B data to a model, $\mathbf{q}(x)=q_1,q_2,\ldots,q_m$, that depends on m collectives variables, which are considered potentially useful descriptors. The collective variables are evaluated at each stored point where the p_B value is known.

A simple model of the reaction coordinate is favored in which the response variable p_B may be related to m collective variables:

$$\lambda(q) = p_B(q) = \sum_{k=1}^{m} \beta_k q_k + q^T \mathbf{A} q + \beta_0 + \varepsilon. \tag{6}$$

This kind of model is called a *response surface model* with m regressor variables.[25] The parameters β_j, $j=0,1,\ldots,m$, are called the regression coefficients and absorb the units from the collective variables, so the reaction coordinate is dimensionless. β_j represents the expected change in λ per unit in q_j when all the remaining independent variables q_i $(i\neq j)$ are held constant. The β_0 parameter allows the reaction coordinate to shift so the transition states are located at $\lambda(q)=\frac{1}{2}$. Interactions between collective variables are included by the cross quadratic term in Eq. (6) where $\mathbf{A}$ is a matrix of adjustable parameters.

The use of a model like that of Eq. (6), however, may not be sufficiently flexible to describe the shape of the $p_B(\lambda)$ function. As illustrated in Fig. 1(b), even if $p_B(\lambda)$ is nearly a linear function over some intermediate range of λ, it will necessarily have a $p_B=0$ plateau for λ in the A basin and a $p_B=1$ plateau for λ in the B basin. Hence, it is convenient to perform the fitting of the model in Eq. (6) to the p_B history data disregarding configurations with $p_B=0$ and $p_B=1$. In this way, the optimized order parameter obtained from our method will only be suitable for estimating p_B values for configurations that lie in the phase space between the two stable states. Because the model surface is not bound to lie in $[0, 1]$ all states with a $p_B\leqslant 0$ can then be enclosed together, defining the initial basin of attraction A with $p_B=0$. Likewise, region B can be defined by enclosing all states with $p_B\geqslant 1$ and assigning them a nominal $p_B=1$. This procedure avoids problems that could result from the fitting of p_B history data containing a large number of states with $p_B=0$ or 1; in such a case, the resulting p_B model would mainly try to fit the plateau regions of the two stable states.

The regression coefficients in Eq. (6) are determined (i.e., model fitting) by standard LSE. The method of which chooses the β so that the sum of the squares of the errors, ε (i.e., uncorrelated random variable error), is minimized.[25] The adequacy of the model fit is then checked by performing an ANOVA that will determine if there is a statistically significant correlation between the response variable p_B and the subset of the collective variables, $\mathbf{q}(x)=q_1,q_2,\ldots,q_m$. The ANOVA involves first the partitioning of the total sum of squares SS_T into a sum of squares due to the model (or the regression) $\mathrm{SS}_R(\beta_j)$ and a sum of squares due to residual (or error) SS_E, and then the testing of the null hypothesis H_0: $\beta_1=\beta_2=\cdots=\beta_m=0$ by computing[25]

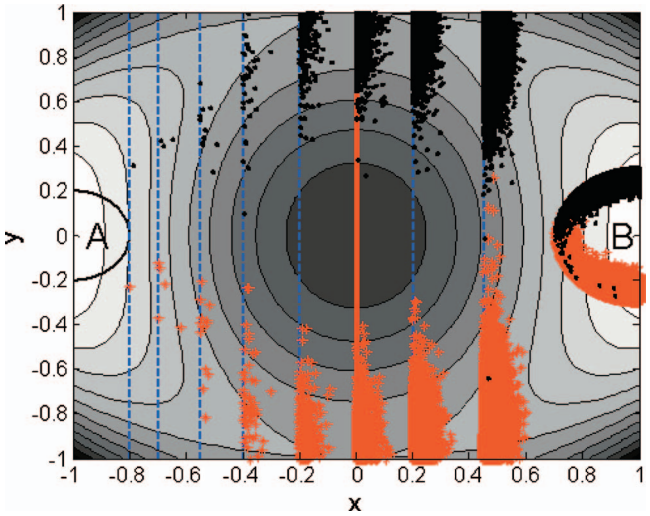

FIG. 2. (Color) Contour graph of $V_1(x,y)$. The color scheme changes from highest (black) to lowest (white) elevations. The initial and final regions are shown by the circles labeled A and B, respectively. The initial guess $\boldsymbol{\lambda}$ vector for the FFS-type simulation is shown by the dotted lines (blue). The thick line (red) shows the TS dividing surface. Two branched paths are also shown: (●) black and (*) red. These state points were used to determine the p_B history for the reaction coordinate estimation.

$$F_0 = \frac{\mathrm{SS}_R(\beta_j)/k}{\mathrm{SS}_E/(n-k-1)} = \frac{\mathrm{MS}_R}{\mathrm{MS}_E}, \tag{7}$$

where k denotes the degrees of freedom (df) for the model, $n-k-1$ is the degrees of freedom for the residual, MS_R is the mean square for the model, MS_E is the mean square for the residuals, and n is the total number of observations for p_B history. H_0 is rejected if F_0 exceeds $F_{\alpha,k,n-k-1}$ or alternatively if the P value for the statistics F_0 is less than α (here chosen to be 0.05 for a 95% confidence interval). The P value of an observed F value is the probability that, given that the null hypothesis is true, the random variable being tested will assume an F value equal or smaller than the observed F_0.[25] Individual regression coefficients are also tested to determine which collective variables are significant for the model description. Adding a variable to the regression model often causes the SS_R to increase and the SS_E to decrease. However, we must decide whether the increase in the SS_R is sufficient to warrant keeping the additional variable in the model. To this end, a null hypotheses H_0: $\beta_j=0$ for testing the significance of any individual regression coefficient is evaluated by a partial F test:[25]

$$F_0 = \frac{\mathrm{SS}_R(\beta_j|\beta_{i\neq j})/1}{\mathrm{MS}_E}, \tag{8}$$

where $\mathrm{SS}_R(\beta_j|\beta_{i\neq j}) = \mathrm{SS}_R(\beta) - \mathrm{SS}_R(\beta_{j\neq i})$ is the regression sum square due to β_j given that $\beta_{i\neq j}$ coefficients are already in the model. H_0 is rejected if F_0 exceeds $F_0 > F_{\alpha,1,n-k-1}$ or alternatively if the P value for the F_0 statistics is less than α. The new order parameter (or reaction coordinate) describes a hyperplane in the space of the significant collective variables $\{q_i\}$ for the p_B surface response. Moreover, because the model fitting uses information from the full range of p_B values, the reaction coordinate should apply to all path regions where p_B values were collected.

Our approach is different from typical approaches,[20,22,23] in which trial reaction coordinates are first proposed and then tested. In those approaches, a good reaction coordinate is found by first selecting combinations of order parameters (based on physical intuition) and then testing them for their ability to describe transition states via additional dynamical simulations. Unlike these approaches[20,22,23] but in analogy with Peters and Trout's[19] approach, our method allows additional variables to be tested without sampling new trajectories or configurations on a constraint surface. Any such new variable is simply calculated at each of the stored points obtained from the initial FFS-type simulation. The major difference with Peters and Trout's[19] method is that their approach uses maximum likelihood estimation (MLE) to seek the probability distribution function (PDF) that makes the observed $p(\mathrm{TP}|x)$ or $p_B(x)$ data most likely. However, application of MLE requires knowledge of the PDF of the data under each proposed model.[26] To this end, they used the aimless shooting algorithm to generate most shooting points (i.e., p_B history) near the unknown $p_B = \frac{1}{2}$ surface.[19] This allowed them to assume a PDF model for the $p(\mathrm{TP}|x)$ or $p_B(x)$ data which was then used to calculate the likelihood of the model given the shooting data. In our approach, since we do not know the PDF for the FFS-type simulation data, LSE is more convenient for the estimation of parameters in Eq. (6).[26]

The entire process described here for obtaining an optimized order parameter can be repeated, so that the current best model is used to generate additional p_B data to be LSE-fitted to the model in Eq. (6) and then get a better estimate of the reaction coordinate, and so on, until some convergence criterion is met. For the simple systems analyzed in this work, however, one iteration of the process was deemed sufficient.

IV. RESULTS

A. Example 1: Analytical potential energy surfaces

Here we apply the FFS-LSE method to find reaction coordinates and transition paths in two simple systems involving a particle moving on a two-dimensional potential energy surface. These model surfaces provide a convenient test bed to validate the proposed method because the stable states and transition states are visually identifiable and known *a priori*.

The first model system is defined by the energy potential

$$V_1(x,y) = \lfloor 4(1-x^2-y^2)^2 + 2(x^2-2)^2 + ((x+y)^2-1)^2 + ((x-y)^2-1)^2 - 2 \rfloor /6. \tag{9}$$

This model surface has been used previously to test transition path sampling methods.[10] A contour graph of this energy landscape is shown in Fig. 2. The potential surface shows two well defined minimum at $(-1,0)$ and $(1, 0)$. The initial and final regions were defined by circles centered at the minima, with a radius of 0.2 and 0.3, respectively. The kinetics of the system was simulated using MC dynamics at $\beta = 1/k_B T = 8$. The move set entailed the sampling in each dimension of a normal distribution centered on the current point:

$$\eta(x_\alpha, x_{\alpha'}) = \frac{1}{\sigma\sqrt{2\pi}} e^{[-(x_\alpha - x_{\alpha'})^2/2\sigma^2]}, \tag{10}$$

where $\sigma = 0.04$ is the standard deviation, chosen according to the distance the particle is expected to travel due to diffusion. The starting points for the FFS-type simulations were randomly sampled from inside region A. The initial guess of order parameter for the BG simulations is given by

$$\lambda_i = \begin{cases} x, & i \neq n = B \\ 1 - 0.5\sqrt{(x-1)^2 + y^2}, & i = n = B \end{cases}. \tag{11}$$

Accordingly, we defined $\lambda_0 = x = -0.80$ and the final region by taking $\lambda_B = \lambda_n = 1 - 0.5\sqrt{(x-1)^2 + y^2} = 0.85$. Note that we used the same definitions for the initial and final regions as in previous works.[10] We used eight interfaces to partition the phase space $(n=8)$ positioned at $\lambda_i (0 \leqslant \lambda_i \leqslant n)$: $\boldsymbol{\lambda}(x) = \{-0.80, -0.70, 0.55, -0.40, -0.20, , 0.00, 0.20, 0.45, 0.85\}$. The number of trials per point at λ_i was $k_i = \{100, 40, 20, 10, 10, 5, 4, 4\}$ $(0 \leqslant i < n)$. Figure 2 also shows the $\boldsymbol{\lambda}$ vector surface and typical transition paths obtained from two independent FFS-type simulations.

Since for this model system the transition state (TS) dividing surface is known *a priori* (dark/red thick line in Fig. 2), we can directly test if our proposed approach leads to the estimation of an optimal order parameter (i.e., p_B surface) having a value of $\frac{1}{2}$ on this TS dividing surface. The p_B history was obtained from the TPE by the method outlined in Sec. III A and fitted to a tentative regression model, including two collective variables (i.e., x and y coordinates) and an interaction term (xy):

$$\lambda(x, y) = \beta_1 x + \beta_2 y + \beta_3 xy + \beta_0. \tag{12}$$

Since there is no curvature in the system (i.e., TS dividing surface is represented by a straight line), polynomial terms of higher degree (e.g., x^2 and y^2) were excluded from the model. Table I shows the LSE parameters and ANOVA for the reaction coordinate model of this system. The P value in Table I for the F statistics of the model [Eq. (12)] is very small, indicating that at least one of the three variables has a nonzero regression coefficient. Table I also reports the F statistics for the test of lack of fit. This test partitions the SS_E into two components, $\mathrm{SS}_E = \mathrm{SS}_{\mathrm{PE}} + \mathrm{SS}_{\mathrm{LOF}}$, where $\mathrm{SS}_{\mathrm{PE}}$ is the sum of squares due to pure error and $\mathrm{SS}_{\mathrm{LOF}}$ is the sum of squares due to lack of fit. $\mathrm{SS}_{\mathrm{PE}}$ is obtained by computing the corrected sum of squares of the repeated observations at each

TABLE I. LSE parameters and analysis of variance for the reaction coordinate model of the two-dimensional energy surface $V_1(x,y)$.

Source	Sum of squares	df	Coefficient	Mean square	F value	P value
Model	405.2	3		136.1	5 669	<0.0001
X (β_1)	405.1	1	0.856	405.1	16 878	<0.0001
Y (β_2)	0.0543	1	0.002	0.0543	2.26	0.1328
XY (β_3)	0.0325	1	0.010	0.0325	1.35	0.2453
Constant (β_0)			0.503			
Residual	518.5	21 894		0.024		
Lack of fit	517.8	21 870		0.024	0.83	0.7765
Pure error	0.70	24		0.029		
Corr. total	923.7	21 897				

level of the collective variables ($\boldsymbol{q}$) and then pooling over the m levels of $\boldsymbol{q}$.[25] Therefore, to test for lack of fit, we would compute the F_0 test statistics and conclude that the regression function is not valid if $F_0 > F_{\alpha,m-k,n-m}$. Since the P value for the F statistics of lack of fit in Table I is very high, we conclude that the model is significant. The upper portion of this table also gives the LSE of each parameter, the partial F-value statistics, and the corresponding P value. As expected, the partial F test shows that the x coordinate is the only important collective variable for the description of the model. Therefore, the reaction coordinate for this particular energy surface only depends on the x coordinate (i.e., P value <0.0001). A second LSE was performed by considering in the reaction coordinate model the x regressor only:

$$\lambda(x) = p_B(x) = 0.504 + 0.853x. \tag{13}$$

Figure 3 shows the p_B contours for the optimal reaction coordinate given by Eq. (13). The optimal λ gives a reaction coordinate surface with a $p_B \sim \frac{1}{2}$ when $x=0$; the energy contours in this figure are shown only to illustrate that the method identifies the correct TS dividing surface $[\lambda(x) = p_B(x) = \frac{1}{2}]$. Note that those states below the $p_B=0$ committor surface simply commit to the initial basin A. Likewise, all those states above the $p_B=1.0$ surface simply commit to the final region B. This example illustrates that our method is successful in identifying an optimal order parameter [i.e., $\lambda(\boldsymbol{q})$] and the correct transition state at $\lambda = p_B = \frac{1}{2}$.

A second more complicated energy potential surface was also used to test our method:[27]

$$V_2(x,\ y) = -e^{-((x-1)^2+y^2)} - e^{-((x+1)^2+y^2)} + 5e^{-0.32(x^2+y^2+20(x+y)^2)} + \frac{32}{1875}(x^4+y^4) + \frac{2}{15}e^{-2-4y}. \tag{14}$$

A contour plot of the potential is given in Fig. 4. This potential surface shows the characteristics of a bistable potential with two minima at (−0.98, 0.06) and (0.96, 0.06) and one saddle point at (−1.96, 1.96). Note that if we were to assume that x is the only important variable and integrate out all the other degrees of freedom (in this case y), then the free-

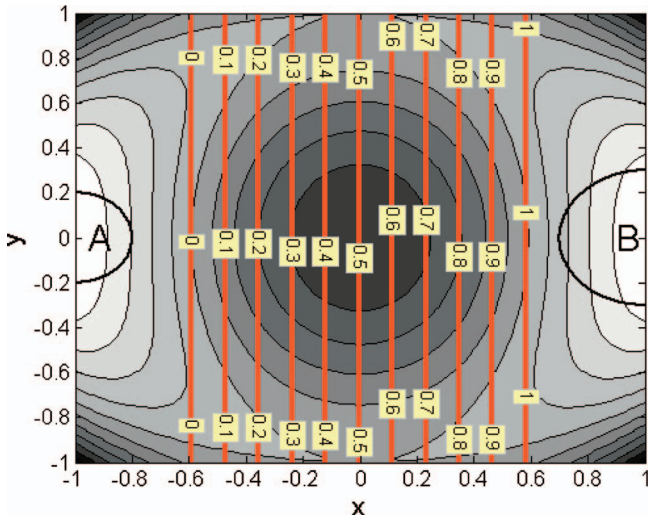

FIG. 3. (Color) Estimated reaction coordinate isolines for model system $V_1(x,y)$. The thick lines (red) are the predicted p_B committors from LSE. The committor values appear as labels over the lines. The contour of the free-energy surface $V_1(x,y)$ is shown only for reference. The color scheme changes from highest (black) to lowest (white) elevations.

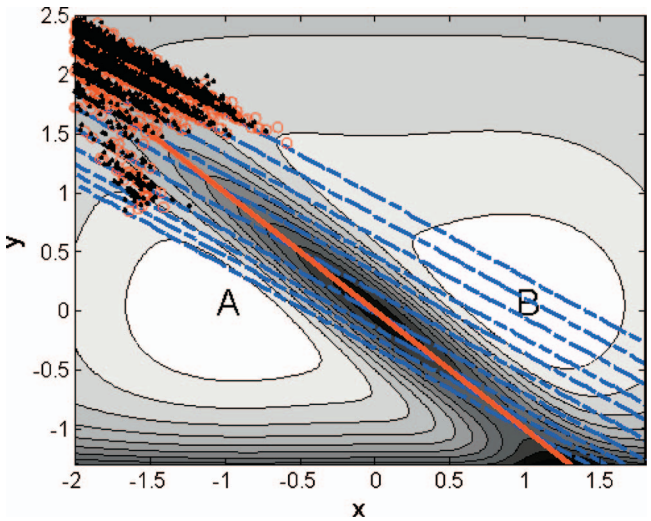

FIG. 4. (Color) Contour graph of $V_2(x,y)$. The color scheme changes from highest (black) to lowest (white) elevations. The initial and final regions are labeled as A and B, respectively. The initial guess $\boldsymbol{\lambda}$ vector for the FFS-type simulation is shown by the dotted lines (blue). The thick line (red) shows the TS dividing surface. Two branched paths are also shown: (●) black and (○) red. These state points were used to determine the p_B history for the reaction coordinate estimation.

energy maximum (along x) would not be located at the saddle point of the surface. Further, to go over the barrier, a particle would have to first move in the opposite direction. Therefore, the optimal reaction coordinate that describes the system's dynamics is expected to depend on both coordinates (x and y) and be a nearly linear function of them in order to describe correctly the TS dividing surface (dark/red thick line in Fig. 4). Hence, the initial guess of order parameter for the FFS-type simulation was assumed to be

$$\lambda(x, y) = 0.268 + 0.807x + 1.164y. \quad (15)$$

This $\boldsymbol{\lambda}$ surface was chosen such that it has a p_B value different from $\frac{1}{2}$ at (0, 0) and the saddle point. We expected that in this case our approach will produce an improved reaction coordinate with the correct regressor coefficients, leading to a slope change of the initial λ isocontours and a displacement to $\lambda(\boldsymbol{q})=\frac{1}{2}$ at the TS dividing surface. Figure 5 shows the $\boldsymbol{\lambda}$ vector surface and typical transition paths obtained from the BG simulations. We used nine interfaces to partition the phase space ($n=9$) positioned at λ_i ($0 \leqslant i \leqslant n$): $\boldsymbol{\lambda}(x,y) = \{-0.10, 0.00, 0.10, 0.25, 0.45, 0.65, 0.80, 1.00, 1.20, 1.40\}$. The number of trials per point at λ_i was $k_i = \{100, 40, 20, 10, 10, 5, 4, 4\}$ ($0 \leqslant i < n$). The kinetics of the system was also studied using MC dynamics at $\beta = 1/k_B T = 6$ and the same move set defined by Eq. (10). The p_B history was obtained from the TPE and fitted to the tentative regression model of Eq. (12). Table II shows the LSE parameters and ANOVA for this case. Since the P value for the test of lack of fit is high, the regression model can be used to describe the variability of the data with a least one of the three collective variables having a nonzero regression coefficient (i.e., P value <0.0001 for F value of the model). As expected, the optimized reaction coordinate for this particular energy surface depends on both coordinates:

$$\lambda(x, y) = p_B(x, y) = 0.616 + 1.153x + 0.941y - 0.109xy. \quad (16)$$

Figure 5 shows the p_B contours for this optimal reaction coordinate. The energy contours in this figure are shown only to illustrate that the method identifies the correct TS dividing surface $\left[\lambda(x,y)=p_B(x,y)=\frac{1}{2}\right]$.

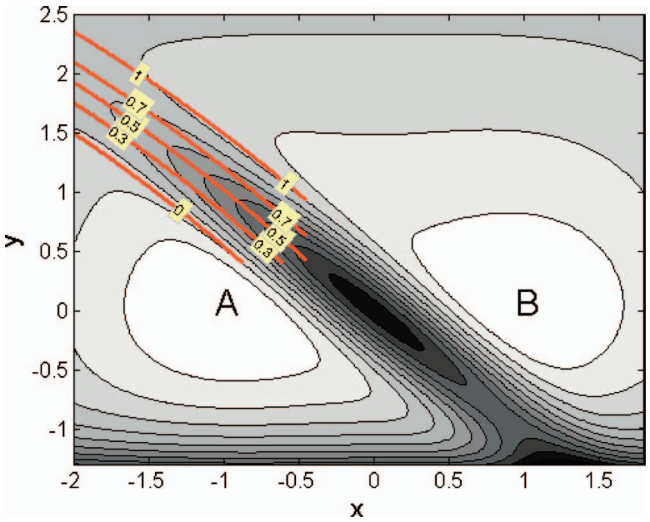

FIG. 5. (Color) Estimated reaction coordinate isolines for model system $V_2(x,y)$. The thick lines (red) are the predicted p_B committors from LSE, whose values appear as labels. Contour of the free-energy surface $V_2(x,y)$ is shown only for reference. The color scheme changes from highest (black) to lowest (white) elevations.

B. Example 2: Genetic switch

This case illustrates the use of our approach for calculating reaction coordinates for a nonequilibrium, rare-event process. The system is a set of chemical reactions for a model symmetric bistable genetic switch whose dynamics do not obey detailed balance. This system has been used previously to test FFS sampling methods.[2,18] The switch consists of a piece of DNA containing two genes A and B, and an operator site (O). The two genes encode for proteins A and B, which can dimerize and bind to the operator site in their homodimer form. However, only one dimer can be bound to DNA (i.e., operator site) at any time, controlling protein production. That is, when A_2 is bound to O, A is produced at rate k, but B is not produced. Likewise, when B_2 is bound to O, B is produced at rate k, but A is not produced.

The FFS-type simulations were carried out using the Gillespie algorithm,[5] which is a widely used kinetic Monte Carlo scheme for propagating chemical reactions. A description of the reactions involved and rate constants for this genetic switch are given in Table III.[2,18]

TABLE II. LSE parameters and analysis of variance for the reaction coordinate model of the two-dimensional energy surface $V_2(x,y)$.

Source	Sum of squares	df	Coefficient	Mean square	F value	P value
Model	6 558	3		2186	99 361	<0.0001
X (β_1)	96.49	1	1.153	96.49	4 386	<0.0001
Y (β_2)	6 364	1	0.941	6364	289 268	<0.0001
XY (β_3)	97.45	1	–0.109	97.45	4 430	<0.0001
Constant (β_0)			0.616			
Residual	4 700	210 530		0.022		
Lack of fit	4 695	20 825		0.023	1.00	0.5123
Pure error	5.33	228		0.023		
Corr. total	11 258	210 533				

TABLE III. Reactions involved for the genetic switch. Forward and backward rate constants k_f and k_b are also given (Refs. 2 and 18).

Protein A	Protein B	k_f	k_b
$2A \leftrightarrow A_2$	$2B \leftrightarrow B_2$	$5k$	$5k$
$O+A_2 \leftrightarrow OA_2$	$O+B_2 \leftrightarrow OB_2$	$5k$	k
$O \rightarrow O+A$	$O \rightarrow O+B$	k	
$OA_2 \rightarrow OA_2+A$	$OB_2 \rightarrow OB_2+B$	k	
$A \rightarrow \emptyset$	$B \rightarrow \emptyset$	$0.25k$	

In previous studies, the order parameter was chosen to be $\lambda = N_B - N_A$, where N_A is the total number of A proteins, and N_B is the total number of B proteins.[2,18] The probability distribution $P(\lambda)$, shown in Fig. 3(b) of Ref. 18, shows that there are two well defined steady states. Therefore, we anticipate that this order parameter should describe well the reaction coordinate, leading to an efficient sampling of pathways. To show that our approach leads to the estimation of an optimal order parameter, we chose a different definition of λ as initial guess for the BG simulations, namely, $\lambda = -N_A$. We defined phase-space region A by taking $\lambda \leqslant -24$ and B by $\lambda \geqslant -4$. The phase space was partitioned with nine interfaces $(n=9)$ positioned at λ_i $(0 \leqslant \lambda_i \leqslant n)$: $\boldsymbol{\lambda}(N_A) = \{-24, -22, -20, -18, -15, -12, -10, -8, -6, -4\}$. The number of trials per point at λ_i was $k_i\{100, 20, 20, 10, 10, 8, 6, 6, 4\}$ $(0 \leqslant i < n)$. The p_B history was obtained from the TPE and fitted to the tentative regression model with two regressor coefficients for N_A and N_B and an interaction term [see Eq. (12)]. Table IV summarizes the LSE parameters and ANOVA for the reaction coordinate model of this system. The ANOVA shows that the regression model can be used to describe the variability of the data with statistically significant regression coefficients for the collective variables N_A and N_B (i.e., P value <0.0001 for partial F-value statistics). Since the P value for the test of lack of fit is high, the model is deemed significant. Figure 6 shows the $\boldsymbol{\lambda}$ response surface for the optimal order parameter projected into N_A and N_B coordinates:

$$\lambda(N_A, N_B) = p_B(N_A, N_B) = 0.500 - 0.038N_A + 0.039N_B. \tag{17}$$

The free-energy landscape in this figure is shown only to illustrate that the method identifies the TS dividing surface $\left[\lambda(N_A, N_B) = p_B(N_A, N_B) = \frac{1}{2}\right]$ that projects onto a line with

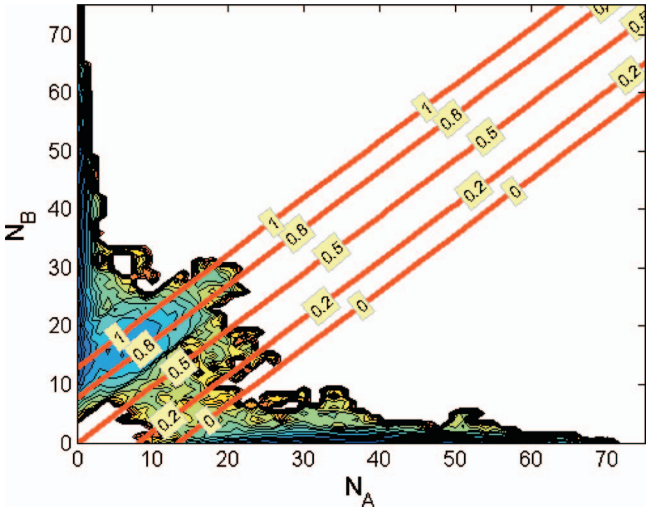

FIG. 6. (Color) Estimated reaction coordinate isolines for the genetic switch model. The thick lines (red) are the predicted p_B committors from LSE, whose values appear as labels. Contour of the free-energy landscape (N_B vs N_A) is shown only for visual reference. The color scheme changes from highest (gray/red) to lowest (black/blue) elevations. The TS dividing surface $\left[\lambda(N_A, N_B) = p_B(N_A, N_B) = \frac{1}{2}\right]$ passes through a line at an $\sim 45°$ angle, with origin at $N_B = N_A = 0$.

$\sim 45°$ slope and origin at (0, 0). Again, as expected, our approach generates an optimized reaction coordinate with similar and oppositely signed regressor coefficients for N_A and N_B. The constant β_0 shifts $\lambda(\boldsymbol{q}) = \frac{1}{2}$ at the TS dividing surface. This example illustrates the applicability of the FFS-LSE approach to an intrinsically nonequilibrium stochastic process (for which some alternative approaches are unsuitable).

C. Example 3: Lattice protein folding

Recently, we applied a FFS-type approach[3] for calculating transition rate constants and for sampling folding paths of a simple cubic lattice protein. The FFS algorithm generated trajectories for the transition between the unfolded and folded states, which were then used to obtain the TSE and the properties that characterize these intermediates. Furthermore, we showed that for this simple system, the fraction of native contacts (Q) is a good order parameter that describes the dynamical bottleneck between the folded and unfolded stable states. Now we explore the possibility that our FFS-

TABLE IV. LSE parameters and analysis of variance for the reaction coordinate model of the genetic switch.

Source	Sum of squares	df	Coefficient	Mean square	F value	P value
Model	2890	3		963.4	34 405	<0.0001
N_A (β_1)	1374	1	−0.038	1374	49 061	<0.0001
N_B (β_2)	1516	1	0.039	1516	54 154	<0.0001
$N_A N_B$ (β_3)	0.0857	1	0.0002	0.0857	3.06	0.0803
Constant (β_0)			0.500			
Residual	605.9	21 664		0.0280		
Lack of fit	38.81	1 340		0.0286	1.02	0.3052
Pure error	567.1	20 324		0.0280		
Corr. total	3496	21 667				

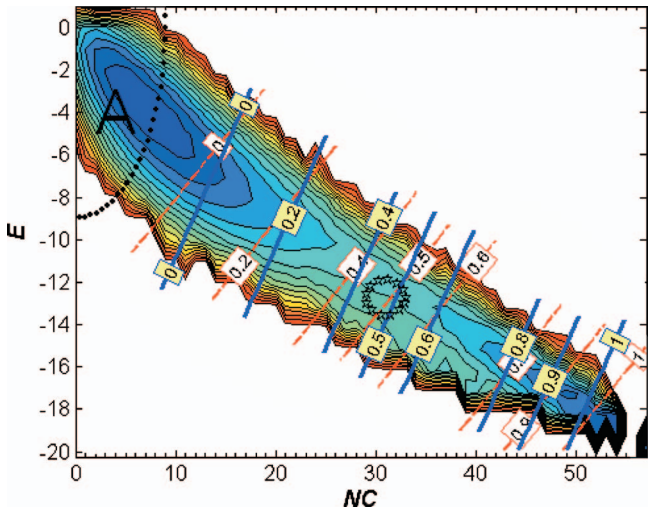

FIG. 7. (Color) Estimated reaction coordinate isolines for the folding of the 48-mer lattice protein model at $T_f=0.27$. The thin dotted lines (red) are the predicted p_B committors from FFS-LSE with $\lambda=\mathrm{NC}$ as initial guess for the order parameter. The thick lines (blue) are the predicted p_B committors from FFS-LSE with $\lambda=-E$ as initial guess for the order parameter. The committor values are shown as labels. Contour plot of the free-energy landscape [energy (E) vs nativeness (NC)] is shown only for visual reference. The color scheme changes from highest (red) to lowest (blue) elevations. The initial region is enclosed by the circle labeled A. The most probable visited transition state region is enclosed by the ellipse with center at ($\mu_{\mathrm{NC}}=31$, $\mu_E=-12.73$).

LSE method could lead to an even better order parameter for this system, allowing a higher computational efficiency for FFS-type simulations and the identification of the TS dividing surface and the TSE without the need to perform additional committor simulations.

The 48-mer protein model adopted here has a unique native structure, that is, a compact structure whose energy is minimum, $-E_{\mathrm{min}}=20.24k_BT$, and has NNC=57 specific or "native" segment-segment contacts. In addition, it exhibits a fast and stable proteinlike folding with a two-state (unfolded-folded) transition.[28] Further details on the model protein, including its structure, thermodynamics, and kinetic behavior, are given elsewhere.[3,28,29]

The folding kinetics of the system was simulated in free space at the corresponding *bulk transition temperature* $T_f=0.27$.[3] Figure 7 shows the contour plot of the free-energy landscape for this system projected over the plane of energy (E) and nativeness, as given by the number of native contacts (NCs); the unfolded state (λ_A) was defined by a circle centered at (NC=0, $E=0$) and radius of 9. The starting points for the FFS simulations were randomly sampled from inside this region A. The folded state was defined by taking $\lambda_B=\lambda_n=\mathrm{NNC}$. The nativeness was used as initial guess of the order parameter (i.e., $\lambda=\mathrm{NC}$) to partition the phase space between the unfolded and folded states for the BG simulations:

$$\lambda_0=\sqrt{\mathrm{NC}^2+E^2}=9, \tag{18}$$

$$\lambda_i=\mathrm{NC}, \quad i>0. \tag{19}$$

We used 12 interfaces to partition the phase space ($n=12$), with interfaces positioned at λ_i ($1\leqslant i\leqslant n$): $\boldsymbol{\lambda}(x)=\{10,12,15,20,26,29,33,37,41,46,51,57\}$. The number of trials per point at λ_i was $k_i=10$ for $0\leqslant i<n$. The p_B history was obtained from the TPE by the method outlined in Sec. III A and fitted to a tentative regression model, including three collective variables: NC, E, and the square radius of gyration R_g^2, and interaction terms between these variables. The ANOVA for this model indicated that the linear terms for NC and E are the only significant ones. The insignificance of the R_g^2 term in the model is expected, because this variable does not help in making a clear distinction between the stable states (e.g., structures from the unfolded basins can also be compact). Thus, a second LSE was performed by only considering in the reaction coordinate model the NC and E regressors, see Table V:

$$\lambda(\mathrm{NC},\ E)=-0.404+0.017(\mathrm{NC})-0.029(E). \tag{20}$$

Table V reports a small and a large P value for the F statistics of the model and the test of lack of fit, respectively. Hence, the reaction coordinate model of Eq. (20) describes the variability of the of the p_B data with statistical significance.

To show that our approach leads to the estimation of a good order parameter regardless of the choice of initial guess for the order parameter, we perform a separate BG simulation with $\lambda=-E$ as the initial order parameter. To make this comparison consistent, we adopted identical definitions for regions A and B, namely, region A was defined by Eq. (18) and region B by taking $\lambda_B=\lambda_n=-E_{\mathrm{min}}=20.24k_BT$ (i.e., minimum energy for the folded state NNC=57). In this case, the phase space between the unfolded and folded states was partitioned with $n=11$ interfaces with λ_0 as in Eq. (18) and

TABLE V. LSE parameters and analysis of variance for the reaction coordinate model of the lattice protein folding with $\lambda=\mathrm{NC}$ as initial guess of the order parameter for the FFS-LSE method.

Source	Sum of squares	df	Coefficient	Mean square	F value	P value
Model	1582	2		790.8	82 371	<0.0001
NC (β_1)	1565	1	0.017	1565	162 566	<0.0001
E (β_2)	16.81	1	−0.029	16.81	1 751	<0.0001
Constant (β_0)			−0.404			
Residual	970.2	100 752		0.0096		
Lack of fit	5.43	626		0.0086	0.90	0.9650
Pure error	964.7	100 126		0.0096		
Corr. total	2552	100 754				

TABLE VI. LSE parameters and analysis of variance for the reaction coordinate model of the lattice protein folding with $\lambda=-E$ as initial guess of the order parameter for the FFS-LSE method.

Source	Sum of squares	df	Coefficient	Mean square	F value	P value
Model	3 185	2		1592	122 026	<0.0001
NC (β_1)	3 175	1	0.021	3175	244 223	<0.0001
E (β_2)	9.87	1	−0.020	9.87	759.2	<0.0001
Constant (β_0)			−0.427			
Residual	12 965	99 322		0.013		
Lack of fit	18.14	4 096		0.004	0.31	1.000
Pure error	1 278	95 226		0.013		
Corr. Total	4 481	99 324				

$$\lambda_i = -E, \quad i > 0, \tag{21}$$

positioned at λ_i $(1 \leqslant i \leqslant n)$: $\boldsymbol{\lambda}=\{9, 10, 11, 12, 13, 14, 15, 16, 17, 18, 20.24\}$. The number of trials per point at λ_i was $k_i = 10$ for $0 \leqslant i < n$. Again, the ANOVA in Table VI indicates that the collective variables for NC and E are the most significant terms in the model:

$$\lambda(\mathrm{NC}, E) = -0.427 + 0.021(\mathrm{NC}) - 0.020(E). \tag{22}$$

The coefficients for the reaction coordinate model [i.e., Eqs. (21) and (22)] obtained from the two independent BG simulations, each based on a different initial guess of the order parameter, are not identical but similar. Furthermore, both simulations consistently disregard the significance of the $\mathrm{NC}\times E$ interaction and R_g^2 terms in the model. Figure 7 shows the $\boldsymbol{\lambda}$ response surface for the optimal order parameter from Eqs. (20) and (22) projected onto the NC and E free-energy landscape. In both cases, the reaction coordinate model identifies the TS dividing surface $[\lambda(\mathrm{NC},E) = p_B(\mathrm{NC},E) = \frac{1}{2}]$, passing through $\mu_{\mathrm{NC}} \approx 31$ (i.e., $Q \approx 0.54$) and $\mu_E \approx -12.73 k_B T$ with a positive linear slope. This value matches well the E value observed at the top of the energy barrier in Fig. 6 of Ref. [3]. The positive slope in the p_B surface indicates that states with lower E for the same NC have a higher probability to commit to the folded state, which is related to the formation of the correct folding foci.[3] Overall, we can state that the FFS-LSE approach leads to good approximations of a reaction coordinate no matter which order parameter is used for the initial phase-space partition in the BG simulations. As indicated in Sec. V B, more iterations of the process could be implemented where in each cycle the current optimized order parameter is used to obtain a new estimate for the reaction coordinate until satisfactory convergence; in this case, just one iteration was enough to get suitable results.

The optimized order parameter expressed as the p_B isocommittor surface leads to new definitions for the A and B regions. Because the model surface is not bound to lie in [0, 1], all states with a $p_B \leqslant 0$ can be enclosed together, defining the initial basin of attraction A. Likewise, region B is defined by enclosing all states with $p_B \geqslant 1$. It can be seen in Fig. 7 that the new definitions of the stable states now more completely enclose the respective basins; these new definitions can then be seen as a refinement with respect to the original ones and a useful by-product of the method. To show that these new definitions for the stable states do not affect the estimation of the average transition rate constant value $(k_{A\to B})$, we compared the $k_{A\to B}$ values for two choices of order parameters: (i) the optimized $\lambda = p_B(\mathrm{NC},E)$ as given by

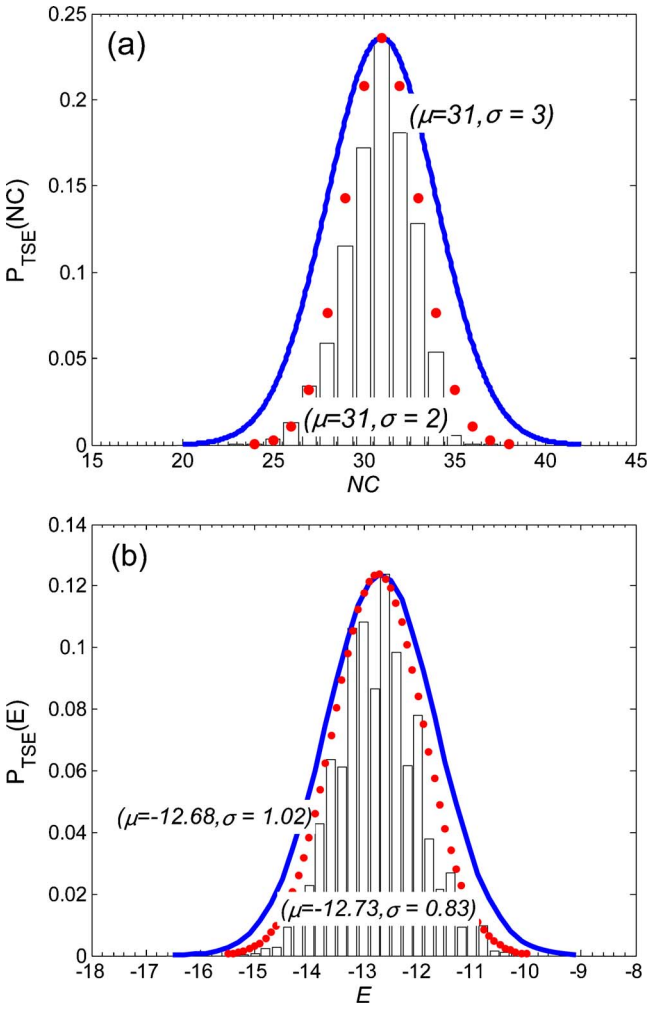

FIG. 8. (Color online) (a) Nativeness (NC) and (b) conformational energy (E) histograms for $p_B(\mathrm{NC},E) = -0.404 + 0.017(\mathrm{NC}) - 0.029(E) = 1/2 \pm 0.1$ surface corresponding to the 48-mer lattice protein model at $T_f = 0.27$. The histograms were accumulated from the states collected in the [0.4, 0.6] surface region during FFS-type simulation (DFFS scheme). The superimposed normal distribution (dotted/red line) that would result from sampling on the exact (μ,σ) surface is also shown. The exact Gaussian distribution obtained from committor analysis is shown by the solid line (blue).

Eq. (20) and (ii) $\lambda=\mathrm{NC}$. In both cases, the DFFS method (see Sec. II A and a brief description in the Appendix) rather than the BG algorithm was used, since the former is most robust to changes in the performance parameters (i.e., in the number of interfaces and of fired trial runs at each λ_i), making it preferable for calculating transition rate constants.[1] For choice (i), the initial region A was defined by $\lambda_0=p_B(\mathrm{NC},E)\leqslant 0$ and the folded state region B was defined by $\lambda_B=\lambda_n=p_B(\mathrm{NC},E)\geqslant 1$. The optimized $\lambda(\mathrm{NC},E)$ of Eq. (20) is only suitable to estimate p_B values for configurations (x) constrained in the phase space between the two stable states, i.e.,

$$p_B(x)=\begin{cases}\lambda(\mathrm{NC},E)=-0.404+0.017(\mathrm{NC})-0.029(E), & 0<\lambda(\mathrm{NC},E)<1.0\\ 0, & \lambda(\mathrm{NC},E)\leqslant 0\\ 1.0, & \lambda(\mathrm{NC},E)\geqslant 1.0.\end{cases} \tag{23}$$

Nine interfaces were used to partition the phase space ($n=9$), with interfaces positioned at λ_i $(0\leqslant i\leqslant n)$: $\boldsymbol{\lambda}(\mathrm{NC},E)=[0.0,0.1,0.2,0.3,0.4,0.5,0.6,0.8,1.0]$. The number of trials at each λ_i was $M_i=1000$ for $0\leqslant i<n$. The statistics were accumulated during 100 blocks where a block consists of a complete DFFS calculation with N_0 starting points. These simulations gave $k_{A\to B}=(8.33\pm0.18)\times10^{-8}$. For choice (ii), when $\lambda=\mathrm{NC}$, we used 12 interfaces spaced in λ_i $(1\leqslant i\leqslant n)$: $\boldsymbol{\lambda}(\mathrm{NC})=[10,12,15,20,26,29,33,37,41,46,51,57]$, $\lambda_0=\lambda_A$ was defined as in Eq. (18), and $\lambda_0=\lambda_B=\mathrm{NNC}$. In this case the DFFS simulations gave $k_{A\to B}=(8.74\pm0.93)\times10^{-8}$. As expected, the redefinition of the stable state regions implied by the reaction coordinate found by FFS-LSE does not affect the average transition rate constant. Note also that the statistical error in the $k_{A\to B}$ estimate is smaller when the optimized order parameter is used to partition the phase space (which correlates with the increase in sampling efficiency to be discussed shortly). Furthermore, we envision that FFS-LSE could be a valuable tool for studying the dynamics in complex systems where the identification of the basins of attraction is more difficult to attain.

We compared our results for the NC distribution within the TSE with those for the protein folding in free space reported in Fig. 9 of Ref. 3. To this end, histograms for NC and E were accumulated from the collection of configurations at the p_B contour of $\frac{1}{2}\pm\sigma$ [i.e., Eq. (20)] during the DFFS simulation (note that configurations from the original BG simulation would be too sparse for this comparison, since the points saved were not at $p_B\sim\frac{1}{2}$). The statistics were accumulated during 50 runs, each one starting from a different random point in region A. The standard error in the computed reaction coordinate model is $\sigma\approx0.1$ (i.e., $\mathrm{MSE}=\sigma^2$), see Table V, and so the $p_B=\frac{1}{2}$ contour includes values in the range [0.4, 0.6]. In Fig. 8, the NC and E distributions found from the TSE reaction coordinate isosurface show Gaussian behavior with mean and standard deviations (μ,σ) of (31, 2) and (−12.73, 0.83), respectively. These mean values of the intrinsic isocommittor surface identify the most populated intermediate regime of rapidly interconverting conformations that are transient and do not accumulate (i.e., sparsely populated). Figure 7 also shows this intermediate region, represented by the ellipse with center at $(\mu_{\mathrm{NC}}=31,\ \mu_E=-12.73)$ and lengths of major and minor semiaxes $\sigma_{\mathrm{NC}}=2$ and $\sigma_E=0.83$, respectively. These mean values match well the average position of the transition state (i.e., $\langle\mathrm{NC}\rangle_{\mathrm{TSE}}=31\pm3$) for the NC distribution determined from a committor analysis;[11] such a $\langle\mathrm{NC}\rangle_{\mathrm{TSE}}$ corresponds to an average conformational energy $\langle E\rangle_{\mathrm{TSE}}\approx-(12.68\pm1.02)k_BT$.

Figure 8 also shows the normal distributions for NC and E obtained from the standard committor analysis.[11] In this analysis, a configuration is considered as a member of the TSE if the interval of confidence $[p_B^{(N)}-\alpha\sigma^{(N)},\ p_B^{(N)}+\alpha\sigma^{(N)}]$ includes the value $\frac{1}{2}$. Here, N is the number of fleeting trajectories used to obtain $p_B^{(N)}$, and $\sigma^{(N)}$ is the standard deviation in the p_B estimate. In these simulations, the confidence level was fixed at $\alpha=1$; more details of the committor analysis are given in Ref. 3. Note that the mean values μ for the NC and E distributions, approximated by the reaction coordinate isosurface, are roughly the same as those of the Gaussian distributions obtained from the committor analysis.[11] Hence, the new optimized order parameter obtained from FFS-LSE can be considered as an appropriate reaction coordinate that describes properly the dynamical bottleneck between the two stable states for this lattice protein system.

Moreover, for a good reaction coordinate, the histogram for the approximate TSE should be closely centered around the characteristic committor value $p_B=\frac{1}{2}$.[11,30] Hence, the quality of the new order parameter from FFS-LSE [i.e., Eq. (20)] can be tested by first collecting states belonging to the TSE from a committor analysis[11] and then calculating the p_B value for those states using the reaction coordinate model. Figure 9 shows the p_B histogram calculated from the model in Eq. (20) for 3674 states belonging to the TSE from a total of 100 branched paths analyzed. The adjusted normal distribution corresponds to $\mu_{p_B}=0.49$ and $\sigma_{p_B}=0.17$. Figure 9 also shows the exact normal distribution $(\mu=\frac{1}{2},\ \alpha\sigma_{p_B}=0.17)$ that would result from sampling on the strict $p_B=\frac{1}{2}$ surface. Note that the committor distribution of the constrained TSE is peaked at $p_B=\frac{1}{2}$, providing a qualitative indicator that the optimized order parameter of Eq. (20) is a good reaction coordinator to describe the system's dynamics. Similar results are obtained if Eq. (22) is used instead of Eq. (20) in the analysis.

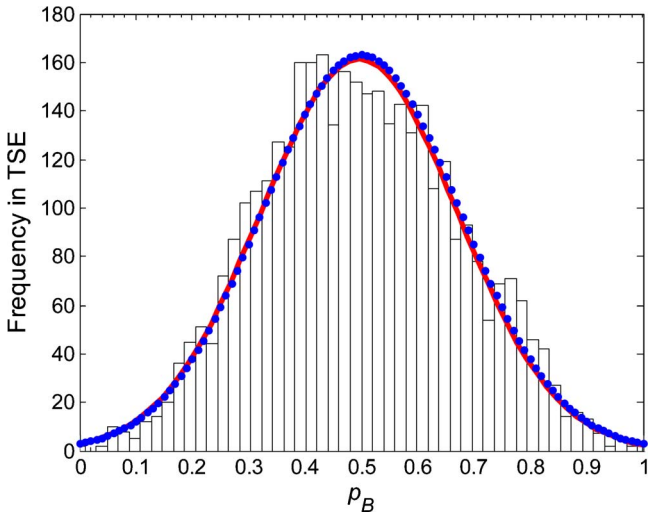

FIG. 9. (Color online) p_B histogram for the states collected at the TSE for the 48-mer lattice protein folding at $T_f=0.27$ from Ref. 3. p_B values were estimated from the reaction coordinate model: $p_B(\mathrm{NC},E)=-0.404+0.017(\mathrm{NC})-0.029(E)$. The bin width is 0.01. The thick line (red) shows the normal distribution ($\mu_{p_B}=0.49$ and $\sigma_{p_B}=0.17$) obtained from the p_B histogram. The exact normal distribution (dotted/blue line) ($\mu=\frac{1}{2}$, $\alpha\sigma=0.17$) that would result from sampling on the exact $p_B=\frac{1}{2}$ surface is also shown. The standard error in the computed reaction coordinate model [Eq. (20)] is $\sigma=0.1$.

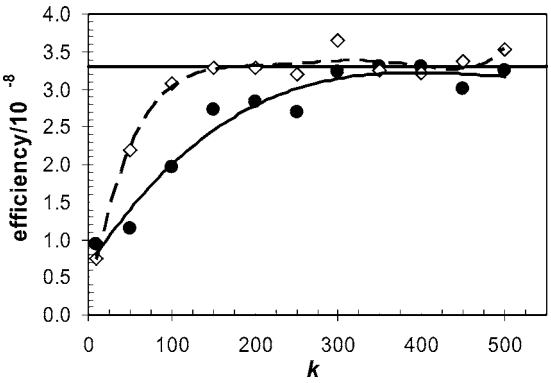

FIG. 10. Measured efficiency ε for the 48-mer lattice protein folding at $T_f=0.27$: (—◇) $\lambda=p_B(\mathrm{NC},E)$ and (—●) $\lambda=\mathrm{NC}$. Simulation results were obtained with 100 DFFS sampling blocks with $N_0=1000$ starting points per block. Interfaces were unequally spaced for $n=9$. The efficiency plateau is marked by the solid horizontal line.

Although the expected value of the transition rate constant does not depend on the definition of λ, a good choice of order parameter is expected to improve the sampling efficiency.[1,2,17] Hence, the choice of λ will determine the optimum (i.e., minimum) number of the interfaces (n) and fired trial runs (k) at each λ_i. Following Allen *et al.*,[1] the computational efficiency (ε) for FFS-type simulations was defined as $1/[C\nu]$ where C represents the computational cost, estimated to be the average number of simulation steps (i.e., MC steps) per block divided by the number of starting points at λ_0. The statistical error ν is defined to be the variance $V[P(\lambda_{n=B}|\lambda_0)]$ in the estimate of $P(\lambda_{n=B}|\lambda_0)$ per initial point at λ_0 divided by the square of the expectation value $E[P(\lambda_{n=B}|\lambda_0)]$:

$$\nu \equiv N_0 \frac{V[P(\lambda_n|\lambda_0)]}{P(\lambda_n|\lambda_0)^2}, \tag{24}$$

where N_0 is the number of starting points at λ_0 and $V[P(\lambda_n|\lambda_0)]=\overline{(P(\lambda_n|\lambda_0))^2}-\overline{(P(\lambda_n|\lambda_0))}^2$. This definition of ε allows us to analyze the efficiency of the order parameter used in the FFS-type simulations in a systematic way.

As indicate before, DFFS is more robust than BG sampling to changes in the k and n parameters, remaining efficient even as k and n become large.[1] Therefore, we compared the ε of the DFFS scheme for the choice of two different order parameters: (i) $\lambda=p_B(\mathrm{NC},E)$ as given by Eq. (20) and (ii) $\lambda=\mathrm{NC}$. Figure 10 shows a comparison of the computational efficiency obtained from DFFS simulations for the protein folding at T_f as a function of k. In these calculations, the same value of k was used for all interfaces: $M_i=k$ for all i. In both cases, the number of interfaces was fixed to $n=9$ because the performance of this algorithm appears to be insensitive to the choice of n as long as it is not too small.[1] To obtain the data in Fig. 10, the nine interfaces were unequally spaced in λ_i $(1\leqslant i\leqslant n)$: $\boldsymbol{\lambda}(\mathrm{NC},E)=\boldsymbol{p}_B(\mathrm{NC},E)$ $\{-0.05,0.0,0.1,0.2,0.35,0.45,0.6,0.85,1.0\}$ and $\boldsymbol{\lambda}(\mathrm{NC})=\{10,12,15,20,26,29,37,46,57\}$. Note that each $\lambda_i(\mathrm{NC},E)$ corresponds to a p_B surface value such that it is crossed midpoint by $\lambda_i(\mathrm{NC})$ (in the NC vs E plane). The value of $\lambda_i(\mathrm{NC},E)=-0.05$ was adopted to ensure that the interfaces were similarly spaced in both cases (even though this value is not meaningful in terms of p_B). The same definitions for the basins of attractions A and B were used to facilitate the comparison: region A is defined by Eq. (18) and the folded state region B by $\lambda_B=\mathrm{NNC}=57$. For each ε estimate, simulations were carried out in a series of 100 blocks with N_0 starting points per block. Each block produces a result $P(\lambda_{n=B}|\lambda_0)$ for the probability to reach B, which is then used to find the variance between blocks $V[P(\lambda_n|\lambda_0)]=\overline{(P(\lambda_n|\lambda_0))^2}-\overline{(P(\lambda_n|\lambda_0))}^2$ where the overbar denotes block averaging.

We observed that as long as k is not too small, its value has little effect on ε. However, when the optimized order parameter is used to partition the phase space, an efficiency plateau ($\sim 3.3\times 10^{-8}$) is reached for smaller k values, i.e., for $k\geqslant 150$ when $\lambda=p_B(\mathrm{NC},E)$ compared to $k\geqslant 300$ when $\lambda=\mathrm{NC}$. Nonetheless, these results must be interpreted with caution, since several important factors are not included in the analysis leading to Fig. 10. Firstly, our analysis does not consider the effect of the number and placement of the interfaces (though very closely spaced interfaces are likely to be computationally inefficient).[1] Secondly, our analysis neglects the effect of correlations between interfaces, though this is justified because neither of the FFS simulations shows a maximum in efficiency as a function of k (i.e., there is memory loss) for the choice of $n=9$ interfaces.[1] In short, we found that the optimized order parameter from the FSS-LSE approach is robust to the choice of k, reaching a computational efficiency plateau at smaller k values than the typical choice of a good order parameter for this system. We envision that this increase in computational efficiency for the FFS-type simulations will be more marked in more complex systems.

Overall this example illustrates that, in contrast to some

previous methods,[9,11,21,22,24] FFS-LSE converges to an optimized order parameter that approaches the true reaction coordinate regardless of the initial trial order parameter. Note also that our approach could avoid problems associated with typical approaches in cases when a proposed reaction coordinate produced a too broad p_B histogram centered at the correct p_B value, indicating that additional candidate variables should be tested via further committor simulations. In our method, the data from the initial FFS-LSE simulation can be reused to screen the additional candidates, which only need to be evaluated at the saved points of the trajectories.

D. Mechanism details from FFS-type algorithm

Since the resulting reaction coordinate model from FFS-LSE corresponds to the p_B surface response, the TSE and hence the mechanistic details of the process can be readily obtained by only analyzing characteristics of the collective variables at the p_B contour of $1/2 \pm \sigma$ (where σ is the desired level of statistical accuracy). To illustrate this, we determined the folding mechanism of a different lattice protein, a model 64-mer protein with the following sequence: *KEKSTAGR VASGVLDSVACGVLGDIDTLQGSPIAKLKTFYGNKFNDVE ASQAHMIRWPNYTLPE*. It also exhibits a single-domain native state with a maximum number of native contacts NNC $=81$ and $E_{\min}=-30.13k_BT$, following an all-or-none transition between two clearly distinguishable states: the native and unfolded states. Folded structures and a detailed thermodynamic characterization for this model protein can be found elsewhere.[31–34] The center of the native structure of this protein presents a large and strong hydrophobic core, which has made this model protein an ideal benchmark for kinetic studies of folding/aggregation dynamics.[31,32]

The FFS-LSE approach was applied to estimate the p_B surface for the folding kinetics in free space at the corresponding transition temperature $T_f=0.27$ (data not shown). Figure 11 shows the contour plot of the free-energy landscape (E vs NC) for this system. NC was used as initial guess of the order parameter (i.e., $\lambda=\mathrm{NC}$) to partition the phase space between the unfolded and folded states in ten interfaces ($n=10$) positioned at λ_i ($0 \leqslant i \leqslant n$): $\boldsymbol{\lambda}(\mathrm{NC}) = \{19,23,28,32,38,45,50,55,60,71,81\}$. Accordingly, the unfolded state (λ_A) was defined by $\lambda_A=\lambda_0 \leqslant 19$ and the folded state by taking $\lambda_B=\lambda_n=81$. The number of trials per point at λ_i was $k_i=10$ for $0 \leqslant i < n$. Projected onto the free-energy landscape, Fig. 11 also shows the $\boldsymbol{\lambda}$ response surface for the optimal order parameter obtained from the FFS-LSE method:

$$\lambda(\mathrm{NC}, E) = -0.733 + 0.022(\mathrm{NC}) - 0.004(E). \qquad (25)$$

Information of the folding mechanism can be obtained by investigating the specific amino acid residues and NC residues that contribute most significantly to the transition state. To this end, histograms for the frequency of each NC pair in the TSE were accumulated from the collection of configurations at the p_B contour of $\frac{1}{2} \pm \sigma$ [i.e., Eq. (25)] during a DFFS simulation. The standard error in the computed reaction coordinate model is $\sigma \approx 0.15$ (i.e., $\mathrm{MSE}=\sigma^2$) and so the $p_B=\frac{1}{2}$ contour includes values in the range [0.35, 0.65].

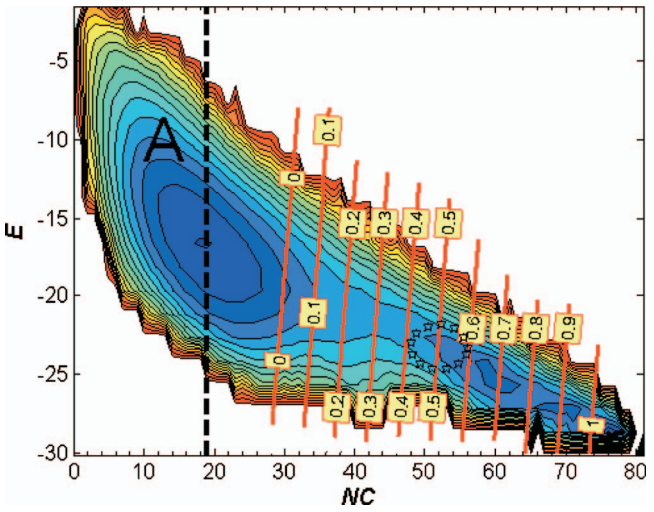

FIG. 11. (Color) Estimated reaction coordinate isolines for the 64-mer lattice protein model folding at $T_f=0.27$. Thin dotted (red) lines are the predicted p_B committors from FFS-LSE, whose values appear as labels. Contour plot of the free-energy landscape [energy (E) vs nativeness (NC)] is shown only for visual reference. The color scheme changes from highest (red) to lowest (blue) elevations. The initial region is delimited by the dotted line labeled A. The most probable visited transition state region is bounded by the ellipse with center at ($\mu_{\mathrm{NC}}=51$, $\mu_E=-23.25$).

The initial region A was defined as $\lambda_A=\lambda_0=p_B(\mathrm{NC},E)=0.0$ and the folded state region B as $\lambda_B=\lambda_n=p_B(\mathrm{NC},E)=1$. The phase space was partitioned with eight interfaces ($n=8$) positioned at λ_i ($0 \leqslant i \leqslant n$): $\boldsymbol{\lambda}(\mathrm{NC},E)=\{0.0, 0.1, 0.2, 0.3, 0.4, 0.5, 0.6, 0.85, 1.0\}$. The number of trials at each λ_i was $M_i=1000$ for $0 \leqslant i < n$ and statistics were accumulated for 100 blocks. The 13 amino acid pairs listed in Table VII are the most probable native contacts that on average have a 90% chance or more to occur in the TSE; they are listed in order of decreasing probability. These results are consistent with those obtained from the TSE found from a committor analysis[11] (data not shown). Figure 11 also shows the most populated intermediate region (given by the $\lambda=0.5$ isosurface) as an ellipse with center at ($\mu_{\mathrm{NC}}=51$, $\mu_E=-23.25$) and lengths of major and minor semiaxes $\sigma_{\mathrm{NC}}=4$ and $\sigma_E=1.42$,

TABLE VII. Most probable native contacts found in the transition state ensemble for 64-mer lattice protein at $T_f=0.27$. They are listed in order of decreasing probability.

NC pairs (i,j)	
i(type)	j(type)
2(E)	35(K)
3(K)	24(D)
3(K)	26(D)
24(D)	37(K)
25(I)	28(L)
25(I)	36(L)
26(D)	35(K)
27(T)	30(G)
27(T)	34(A)
28(L)	33(I)
29(Q)	32(P)
31(S)	34(A)
33(I)	36(L)

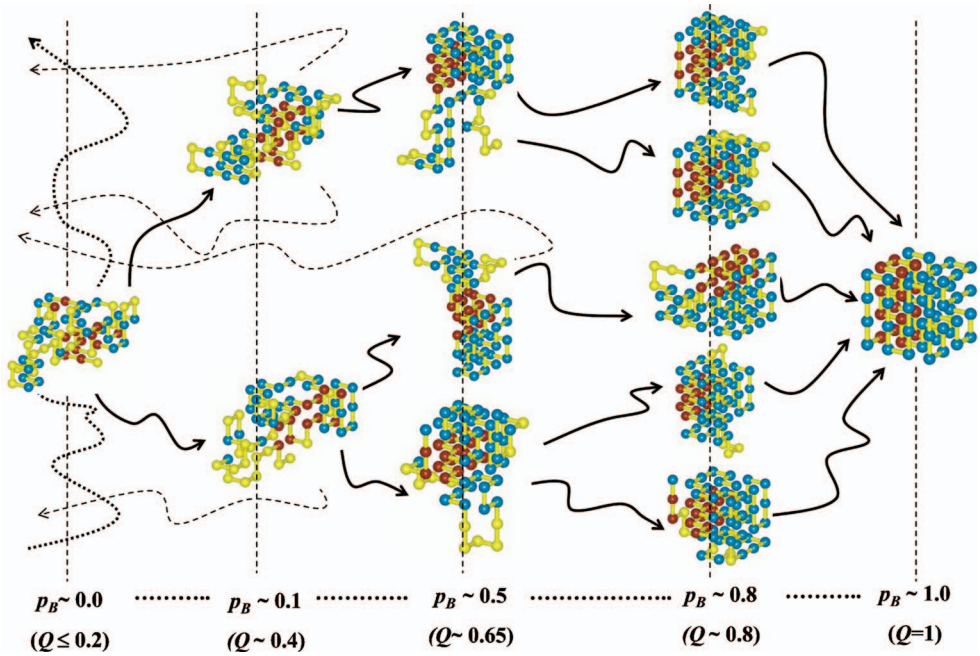

FIG. 12. (Color) Representative snapshots for the folding event of the 64-mer lattice protein at $T_f=0.27$. The simulation trajectory in the unfolded basin is shown by the thick dotted line. Trial runs (k_i) fired from λ_i that successfully reached the next λ_{i+1} interface are shown by the thick line and those which failed to reach λ_{i+1} are shown by the dotted line. Amino acid contacts are coded by the color of the residue: gray/blue indicates native contacts, whereas black/red designates the native contacts listed in Table VII, which have higher probability to belong to the transition state. The final frame shows the native state conformation.

respectively. Notice that the ellipse is a bit off center because of limitation of the FFS-LSE fit and the statistical error in the estimation of the p_B values. Figure 12 shows snapshots of typical folding trajectories for this protein; it can be observed that the 13 NC pairs with greater occurrence probability in the TSE ($p_B \approx 0.5$, $Q \sim 0.65$) correspond to the nucleus that begins to form at early stages ($p_B \approx 0.1$, $Q \sim 0.2$) during the folding process (the residues are shaded to display the formation of NCs). Note that the darker (red) residues are clustered in a patch, representing a core of NC pairs that is essential for the transition from unfolded to native state and contribute (on average) to 22.2% of the potential energy of the folded structure. This nucleation scenario is consistent with that previously reported in experimental[35,36] and simulation[3,37] studies. In general, the folding mechanism for the lattice protein begins with the peptide chain in a highly fluctuating unfolded state characterized by extended regions that persist up until the TS is reached. It then switches to a series of conformations with a partial, nativelike structure, as indicated by the emergence of a persistent darker (red) patch (i.e., a nucleus of NCs). After that, there is a rapid transition from the partially folded intermediate state to more compact nativelike conformations (at $p_B \approx 0.8$, $Q \sim 0.80$). This transition corresponds to the collapse of fluctuating internal loops in the protein. In the final stage of folding, external loops at the surface of the protein rearrange to attain the folded structure.

V. CONCLUSIONS

How does one identify transition states and a good reaction coordinate for rare events? Answering this ubiquitous question implies finding an ensemble of reactive trajectories (TPE) which is most efficiently found from transition path sampling methods. FFS-type algorithms, for example, can generate transition paths that partially overcome the problem of reaction coordinate selection. However, some of the challenges for the application of these algorithms include the determination of an adequate order parameter to describe transition state regions and the assessment of computational efficiency. In this article, we followed the idea that the best reaction coordinate to describe rare events, in fact the reaction coordinate, consists of the isocommittor p_B surfaces. This idea is not new,[9,11,19,21,22,24] but our approach differs from these previous approaches in that the path sampling is independent of the reaction coordinate to be tested. Thus, the proposed FFS-LSE approach better lends itself to applications in complex systems where the reaction coordinate cannot be identified *a priori*. The FFS-LSE method generates estimates for p_B on the fly from FFS-type simulations using an initial guess of the order parameter. The p_B history is then used to fit a model for the reaction coordinate in terms of several collective variables by LSE, and the significant terms in the model are determined by an analysis of variance. In this way, an optimized reaction coordinate is obtained that depends on a few relevant variables. The collective variables are evaluated at each stored point for which the p_B value is known, so that p_B is calculated only once for a set of states on the TPE. In this work, we used the BG algorithm to estimate the p_B values because in this scheme each point at any interface λ_i is sampled by firing a minimum number (k_i) of trial runs to the next interface, thus ensuring reasonably good statistics for the estimation of p_B values via Eq. (5). However, the DFFS scheme (rather than BG) could also be used to get p_B estimates if one only considers points for which a

minimum number of trials runs have been fired. In general, we envision that the dynamics of a system can be studied via two FFS-type simulations: the first one intended to determine a good reaction coordinate and the second one intended to get mechanistic details of the process kinetics (using the good reaction coordinate found first). In the protein folding examples in this work, we used BG for the first stage and DFFS for the second.

The proposed method was applied to find reaction coordinates and transition states in three simple test examples. The examples of a particle moving on a bistable potential energy surface proved that the method allows the identification of the exact TS dividing surface from the p_B history. The example on the genetic switch shows that FFS-LSE can be applied to the estimation of reaction coordinates for nonequilibrium, rare-event problems. Finally, the example of the lattice protein folding shows that the FSS-LSE method leads to an improved order parameter (relative to other typical good choices), and thus to a higher computational efficiency for FFS-type simulations. Moreover, we showed that the FFS-LSE approach provides a simple way in which information about the transition path ensemble (TPE) and transition state ensemble (TSE) and hence mechanistic details of the dynamics of the system could be obtained while calculating the transition rate constant. Hence, once the TS dividing surface is known, the TSE can be extracted by simply screening the characteristics of the collective variables around the $p_B \sim \frac{1}{2}$ contour during a single FFS-type simulation without the need to perform additional committor simulations.

While the simple examples studied here illustrate the validity and efficiency of the proposed method, in future work we plan to compare its performance with that of other variants, including the ML approach.[19] We argue, however, that the FFS-LSE approach should be seen as a complementary rather than a competing approach to find good reaction coordinates (e.g., for systems with stochastic dynamics or nonequilibrium states for which FFS may be more suitable than TPS). The FFS-LSE method could become a valuable tool for studying the dynamics in complex systems where the identification of a good reaction coordinate is essential for the efficient use of path sampling approaches.

ACKNOWLEDGMENT

Support from the Sloan Foundation and National Science Foundation Award No. BES-0093769 is acknowledged.

APPENDIX THE DIRECT FORWARD FLUX PATH SAMPLING ALGORITHM

The DFFS method is similar to BG with the difference that in DFFS one samples M_i randomly selected points at each λ_i, rather than sampling k_i trial runs per stored point at λ_i. After an equilibration period, a first simulation is performed to store points each time the trajectory leaves A and crosses λ_0. This run in basin A is suspended when N_0 points at λ_0 have been collected. In the second stage of the algorithm, partial paths are generated from this initial configuration stored at λ_0 to estimate the conditional probabilities, $P(\lambda_{i+1}|\lambda_i)$, of reaching λ_{i+1} from λ_1. Starting with the collection of N_0 points at λ_0, M_0 trials runs are fired from randomly selected such points and are continued until either reaching λ_1 or returning to the initial region A. Then, each end-point configuration $N_S^{(0)}$ resulting from successful trial runs to reach λ_1 is stored and used as starting point for M_1 trial runs toward λ_2 (or back to A). If $N_S^{(1)}>0$ of the trial runs reach λ_2, the partial paths are continued by initiating M_2 trial runs to λ_3 from each of the $N_S^{(1)}$ successful configurations. This procedure is repeated using the collection of points generated at previous interfaces and firing trials that run as far as λ_{i+1} or λ_A until either the final region $\lambda_n=\lambda_B$ is reached or because no successful trials were generated at some intermediate interfaces. In this way, an estimated value of $P(\lambda_{i+1}|\lambda_i)=N_S^{(i)}/M_i$ can be obtained for each interface. As with the BG method, $P(\lambda_{n=B}|\lambda_0)$ is obtained by using Eq. (2) and the flux $\bar{\Phi}_{A,0}/\bar{h}_A$ in Eq. (1) is obtained from the simulation run in basin A by dividing the total number of crossing configurations at λ_0 by the total length of this run. For a complete description of the FFS path sampling scheme, the readers are referred to Ref. 2.

[1] R. J. Allen, D. Frenkel, and P. R. ten Wolde, J. Chem. Phys. **124**, 194111 (2006).
[2] R. J. Allen, D. Frenkel, and P. R. ten Wolde, J. Chem. Phys. **124**, 024102 (2006).
[3] E. E. Borrero and F. A. Escobedo, J. Chem. Phys. **125**, 164904 (2006).
[4] D. Chandler, *Introduction to Modern Statistical Mechanics* (Oxford University Press, New York, 1987).
[5] D. Frenkel and B. Smit, *Understanding Molecular Simulation: From Algorithms to Applications*, 2nd ed. (Academic, Boston, 2002).
[6] J. B. Anderson, Adv. Chem. Phys. **91**, 381 (1995).
[7] G. E. Crooks and D. Chandler, Phys. Rev. E **6402**, 026109 (2001).
[8] P. G. Bolhuis, Proc. Natl. Acad. Sci. U.S.A. **100**, 12129 (2003).
[9] P. G. Bolhuis, D. Chandler, C. Dellago, and P. L. Geissler, Annu. Rev. Phys. Chem. **53**, 291 (2002).
[10] C. Dellago, P. G. Bolhuis, F. S. Csajka, and D. Chandler, J. Chem. Phys. **108**, 1964 (1998).
[11] C. Dellago, P. G. Bolhuis, and P. L. Geissler, Adv. Chem. Phys. **123**, 1 (2002).
[12] A. K. Faradjian and R. Elber, J. Chem. Phys. **120**, 10880 (2004).
[13] T. S. van Erp and P. G. Bolhuis, J. Comput. Phys. **205**, 157 (2005).
[14] T. S. van Erp, D. Moroni, and P. G. Bolhuis, J. Chem. Phys. **118**, 7762 (2003).
[15] D. Moroni, T. S. van Erp, and P. G. Bolhuis, Physica A **340**, 395 (2004).
[16] D. Chandler, J. Chem. Phys. **68**, 2959 (1978).
[17] T. S. van Erp, J. Chem. Phys. **125**, 174106 (2006).
[18] R. J. Allen, P. B. Warren, and P. R. ten Wolde, Phys. Rev. Lett. **94**, 018104 (2005).
[19] B. Peters and B. L. Trout, J. Chem. Phys. **125**, 054108 (2006).
[20] R. B. Best and G. Hummer, Proc. Natl. Acad. Sci. U.S.A. **102**, 6732 (2005).
[21] G. Hummer, J. Chem. Phys. **120**, 516 (2004).
[22] A. Ma and A. R. Dinner, Protein Sci. **13**, 219 (2004).
[23] L. Maragliano, A. Fischer, E. Vanden-Eijnden, and G. Ciccotti, J. Chem. Phys. **125**, 024106 (2006).
[24] E. Weinan, W. Q. Ren, and E. Vanden-Eijnden, Chem. Phys. Lett. **413**, 242 (2005).
[25] D. G. Mongomery, *Design and Analysis of Experiments*, 5th ed. (Wiley, New York, 2001).
[26] I. J. Myung, J. Math. Psychol. **47**, 90 (2003).
[27] P. G. Bolhuis, www.science.uva.nl/~bolhuis/tps/content/exercise.pdf (2007).
[28] V. I. Abkevich, A. M. Gutin, and E. I. Shakhnovich, Folding Des. **13**, 221 (1996).
[29] L. M. Contreras, F. Martinez-Veracoechea, P. Pohkarel, A. D. Stroock, F.

Escobedo, and M. P. DeLisa, Biotechnol. Bioeng. **94**, 105 (2006).
[30] B. Peters, J. Chem. Phys. **125**, 241101 (2006).
[31] D. Bratko and H. W. Blanch, J. Chem. Phys. **114**, 561 (2001).
[32] D. Bratko and H. W. Blanch, J. Chem. Phys. **118**, 5185 (2003).
[33] K. Leonhard, J. M. Prausnitz, and C. J. Radke, Phys. Chem. Chem. Phys. **5**, 5291 (2003).
[34] K. Leonhard, J. M. Prausnitz, and C. J. Radke, Biophys. Chem. **106**, 81 (2003).
[35] A. R. Fersht, Proc. Natl. Acad. Sci. U.S.A. **92**, 10869 (1995).
[36] A. R. Fersht, Curr. Opin. Struct. Biol. **7**, 3 (1997).
[37] V. S. Pande and D. S. Rokhsar, Proc. Natl. Acad. Sci. U.S.A. **96**, 1273 (1999).